DISTRIBUTIONS OF LOAD STRESSES AND RESIDUAL STRESSES AT NOTCHES

Soon-Bok Lee*

(Received June 1, 1992)

The fatigue strengh reduction factor K_f can be mitigated or eliminated by suitable surface treatments. Analysis of these effects requires the knowledge of the distributions of load stresses and of residual stresses below the surface of notches. This paper describes a simple, approximate formula to determine load stress distributions and residual stress distributions at notches. The load stress distributions by the present approach were compared with finite element analysis under tension, bending and torsion loading. Residual stress distributions by the simple formula were compared with measured data by shot peening. An example of optimization in surface treatments by such analysis is shown.

Key Words: Load Stress, Residual Stress, Fatigue Notch Factor, Shot Peening, Notch

NOMENCLATURE

a,b,c : Constants in the load stress distribution
d : Total depth to which the compressive residual stress extends (mm)
D : Diameter, Large diameter of filleted shaft (mm)
K_f : Fatigue strength reduction factor, fatigue notch factor
K_t : Stress concentration factor
n : Exponent in the load stress distribution
N_f : Number of cycles to failure
r : Radius of fillet or semi-circular notch (mm)
R : Radius of shaft (mm)
x : Distance from notch root (mm)
w : Half width of fillet or notch in their narrow section (mm)
η : Distance from surface to the point where stress gradient at the surface meets the x-axis (mm)
σ_a : Alternating stress (MPa)
σ_{eq} : Equivalent stress (MPa)
σ_f' : Fatigue strength coefficient (MPa)
σ_F : Fatigue strength (MPa)
σ_L : Load stress at point x (MPa)
σ_m : Mean stress (MPa)
σ_N : Net stress (Mpa)
σ_o : Nominal stress (MPa)
σ_R : Residual stress (MPa)
$\sigma_{R,P}$: Maximum compressive residual stress or peak compressive stress (MPa)
ξ : Half width of the notch in plates or the radius at the narrow section of shafts (mm)

1. INTRODUCTION

Fatigue cracks in structures and components usually start at notches. It is common practice to relate the fatigue behavior of notched parts to the available material data referred to smooth specimens or cracked fracture mechanics specimens.

1.1 The Fatigue Strength Reduction Factor

The theoretical stress concentration factor K_t can be obtained by various analytical and experimental methods or from the literature (Peterson, 1974). It can serve as a first approximation for calculating the fatigue strength of notched parts at fully reversed stresses and long life from the fatigue strength of smooth specimens. The fatigue notch factor (or fatigue strength reduction factor) K_f relates the obvserved behavior of the notched specimen to the data obtained from smooth specimens. Neuber(1946) and Peterson(1974) have correlated the difference between K_f and K_t with the stress gradient. Their formulas relate the stress gradient to the notch radius, regardless of the notch geometry. Siebel and Stieler(1955) have published more detailed data on stress gradient. Schijve(1980) has discussed those formulas and the gradient problem. Berkovitas(1986) discussed the variation of K_f with life time, stress ratio and temperature.

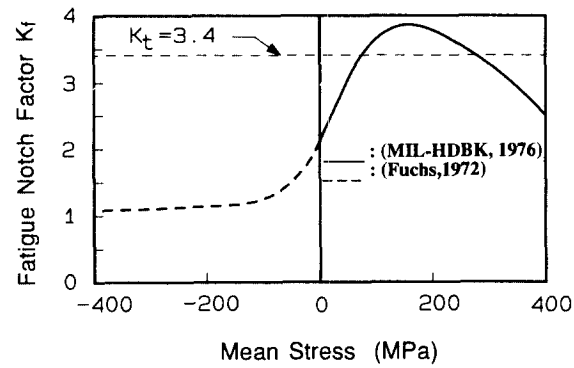

Fig. 1 Fatigue notch factor versus mean stress for 7075-T6 aluminum bar at 10^7 cycles

*Department of Mechanical Engineering, Korea Advanced Institute of Science & Technology, Taejon 305-701, Korea

From the available data (MIL-HDBK-5C, 1976, Fuchs, 1972) it was found that notch factor K_f depends not only on K_t and the stress gradient but very strongly on the mean stress. Tensile mean stress can raise the notch factor K_f far beyond the stress concentration factor K_t. Compressive mean stress can eliminate the notch effect. Fig. 1 shows the long life notch factor for a bar with $K_t=3.4$ plotted as a function of the mean stress. Similar behavior of many materials have been shown by Walker(1970) and Smith et al.(1970). They indicate that fatigue cracks will not grow unless tensile stress is present during some part of the load cycle.

1.2 Strength Enhancement

It has been long known that failures of notched parts can be prevented by certain treatments such as nitrifying, carburizing, surface rolling, or shot peening. Research has shown that the beneficial effect of such treatments depends in large part or entirely on the compressive stresses produced in an shallow surface layer (Almen and Black, 1963). These residual stresses prevent fatigue cracks from growing beyond a small depth (Gerber and Fuchs, 1970). To analyze the action of the beneficial surface treatments and to optimize their application it is necessary to know the distributions of these residual stresses and of the load stresses. This was expressed as early as 1961 by Peterson(1961). With computers available today the consideration of stress distribution is more readily feasible than it was earlier.

2. LOAD STRESS DISTRIBUTIONS

2.1. An Analytical Approach for Load Stress Distributions

The distributions of load stresses may be known, as for thick walled tubes and for holes in wide plates, or they may be computed by finite element methods. For many applications it is sufficient to approximate the load stress distribution by the formula

$$\sigma_L=\sigma_o\left[a+b\left(1-\frac{x}{\xi}\right)+c\left(1-\frac{x}{\xi}\right)^n\right] \tag{1}$$

where σ_o is the nominal stress at the notch root, ξ is the half width of the notch in plates or the radius at the narrow section of shafts, i.e., $\xi=w$ for plates and $\xi=R$ for shafts. The four parameter a, b, c, n in Eq. (1) are calculated to match the stress concentration factor and stress gradient at the surface, and equilibrium with the nominal stress distribution, and stress condition at the center. These calculated parameters are shown in the appendix for various notches and fillets in terms of stress concentration factors K_t and stress gradient intercept η and notch geometry. Fig. 2 defines the coordinates at notches and stress gradient intercept η. The stress gradient intercept η, which is the distance to the point where the slope of the stress distribution meets the x-axis, is obtained as

$$\eta=-\frac{K_t\sigma_o}{\left(\frac{d\sigma_L}{dx}\right)} \tag{2}$$

Stress concentration factors for many notch geometries are available in the literature (Peterson, 1974); stress gradients for a few notch geometries are shown in Table 1 based on the available data (Siebel and Stieler, 1955) in terms of the length η which is defined in Fig. 2. Information on load stress distributions can thus be obtained.

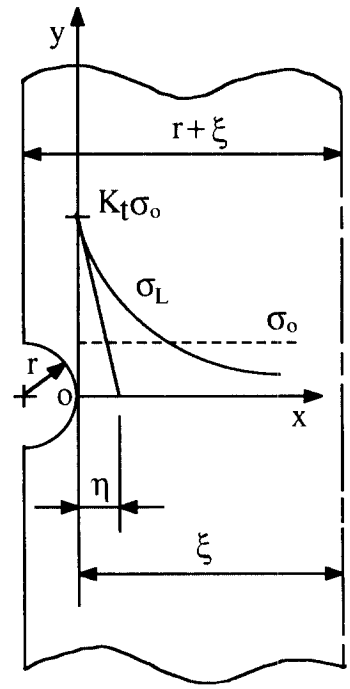

Fig. 2 Definition of η in a notched shaft or in a notched plate $\xi=R$ for shafts and $\xi=w$ for plates

Table 1 Stress gradient intercept η for various type of notched specimen and loading

Type of notched Specimen	Type of loading		
	Tension	Bending	Torsion
Edge notch	$\frac{r}{2}$	$\frac{rw}{r+2w}$	—
Groove	$\frac{r}{2}$	$\frac{rR}{r+2R}$	$\frac{rR}{r+R}$
Fillet	$\frac{r}{2}$	$\frac{r(B+2w)}{2(B+2w+2r)}$	—
Fillet	$\frac{r}{2}$	$\frac{r(D+2R)}{2(D+2R+2r)}$	$\frac{r(D+2R)}{D+2R+4r}$
Central hole	$\frac{r}{2.5}$	$\frac{rB}{2.5B+2r}$	—
Central hole	$\frac{r}{2.5}$	$\frac{rD}{2r+4D}$	$\frac{rD}{2r+3D}$
Central hole	—	—	$\frac{r}{3}$
Key Way	—	—	$\frac{rD}{2r+D}$

2.2 Finite Element Analysis

Finite element analysis was performed to obtain the load stress distributions for the plates or shafts with semi-circular notches and quarter circular fillets and under various loadings. In the load stress distributions, stress concentration

factor, K_t and stress gradient intercept η were obtained with finite element methods. Relative stress gradients of quarter-circular fillets and semi-circular notches were obtained by calculating the slope with two data points of finite element results near the surface.

For the analysis of plates with semi-circular notches in tension, two dimensional multi-node isoparametric solid elements were used. Analysis was performed for various normalized notch radius (i.e., r/w=0.1, 0.125, 0.167, 0.2, 0.333, 0.5, 0.667, 0.833, and 1.0). Fig. 3(a) shows the finite element model of a notched plate with r/w=1 and Fig. 3(b) shows the loading conditions on the notched shaft for the finite element analysis under tension, bending and torsion. Since the shaft is an axisymmetric shape, and the tensile load is also axisymmetric, 2-D multi-node isoparametric solid elements were used for the finite element analysis under tension. Bending or torsion loadings on shafts are the non-axisymmetric load on an axisymmetric model. The plane finite element model as shown in Fig. 3(a) and axisymmetric two dimensional solid elements were used for the analysis under bending and torsion.

The results of finite element analysis on K_t for a shaft with semi-circular notches under torsion and bending and tension, and for a plate with semicircular notches under tension were in good agreement with the formula of Roark and Young(1975). Fig. 4 shows an example of such comparisons. The results of finite element analysis on η for a shaft with semi-circular notches under torsion and bending, and plates with a notch or a fillet in tension are shown in Fig. 5 and they are compared with the formula suggested by Siebel and Stieler(1955) quoted by Klesnil and Lukas(1980). For quarter-circular fillets in plates the ratio of the intercept η to the notch radius is no longer constant when the ratio of notch radius to fillet width becoms small. The same is true for semi-circular notches in plates, as shown in Fig. 5.

Fig. 6 shows the comparisons of load stress distributions by Eq. (1) with the finite element analysis for semi-circular notches (r/w=1) in the plate and shaft under tension, and the shaft under torsion. Load stress distributions by the analyti-

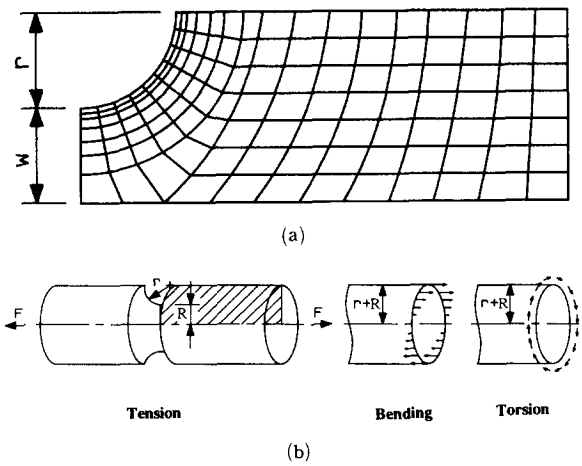

Fig. 3 (a) Finite element model of a notched plate with r/w=1
(b) Loading conditions on the notched shaft for the finite element analysis

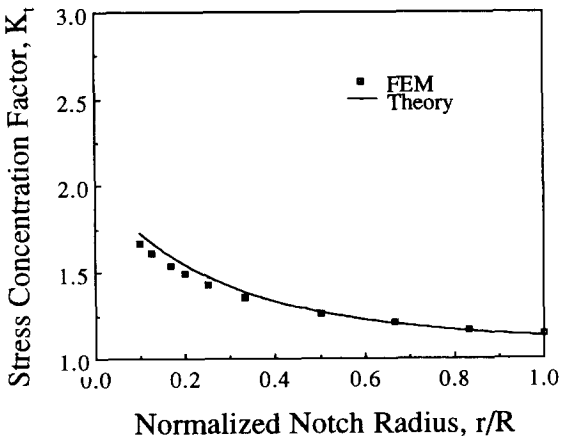

Fig. 4 Stress concentration factors for the shaft with semi-circular notch under torsion

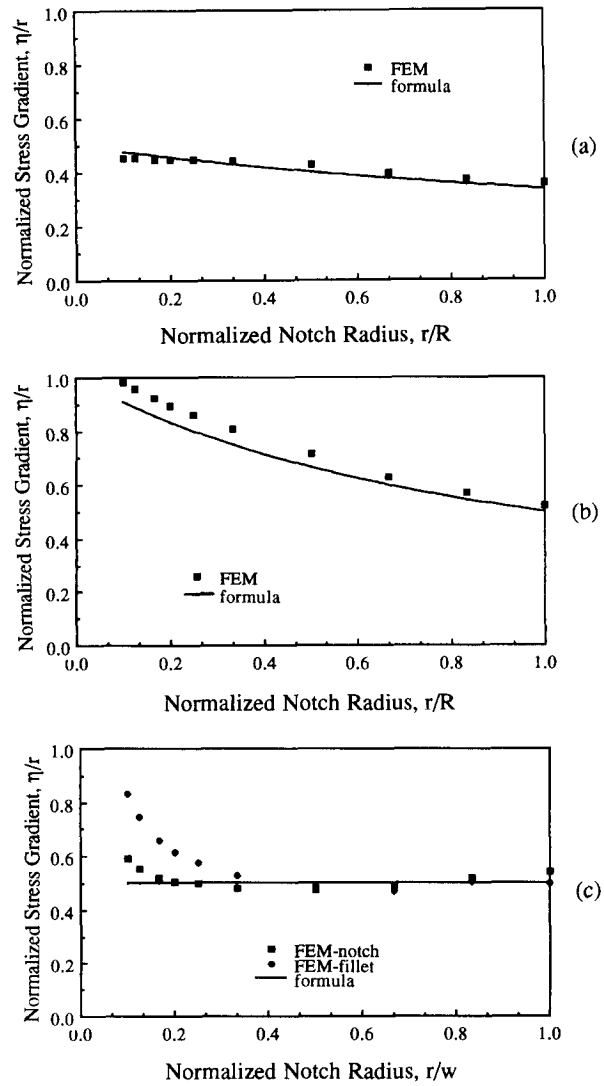

(a) Notched shaft under bending
(b) Notched shaft under torsion
(c) Plate with a notch or a fillet in tension

Fig. 5 Comparison of FEM results and formula taken from Table 1 for stress gradient intercept η of various notches and loadings

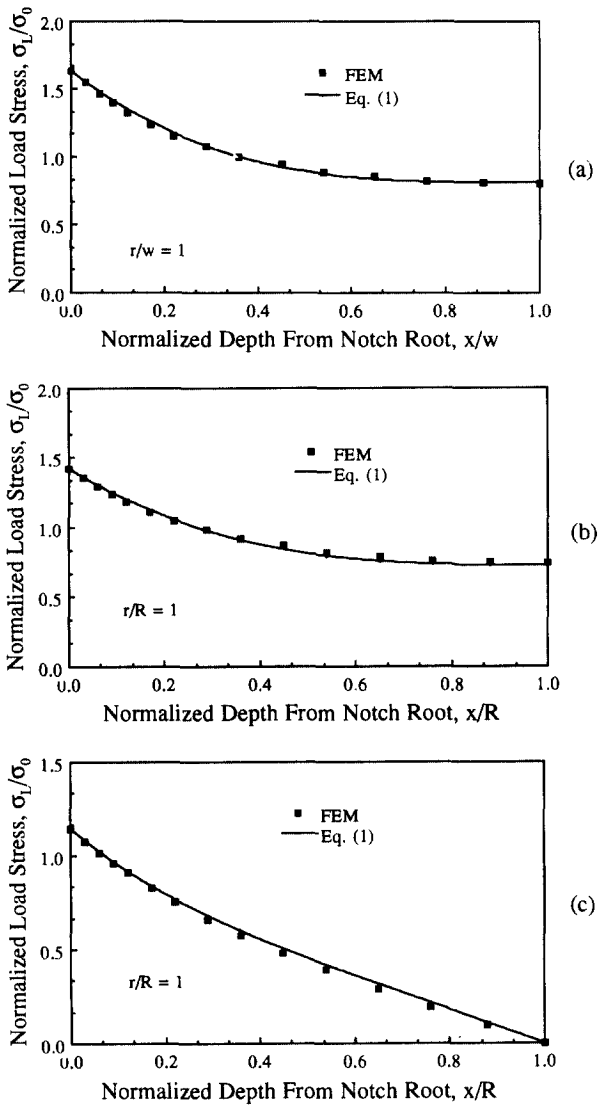

(a) Notched plated under tension
(b) Notched shaft under tension
(c) Notched shaft under torsion

Fig. 6 Comparisons of load stress profiles between Eq. (1) and finite element result

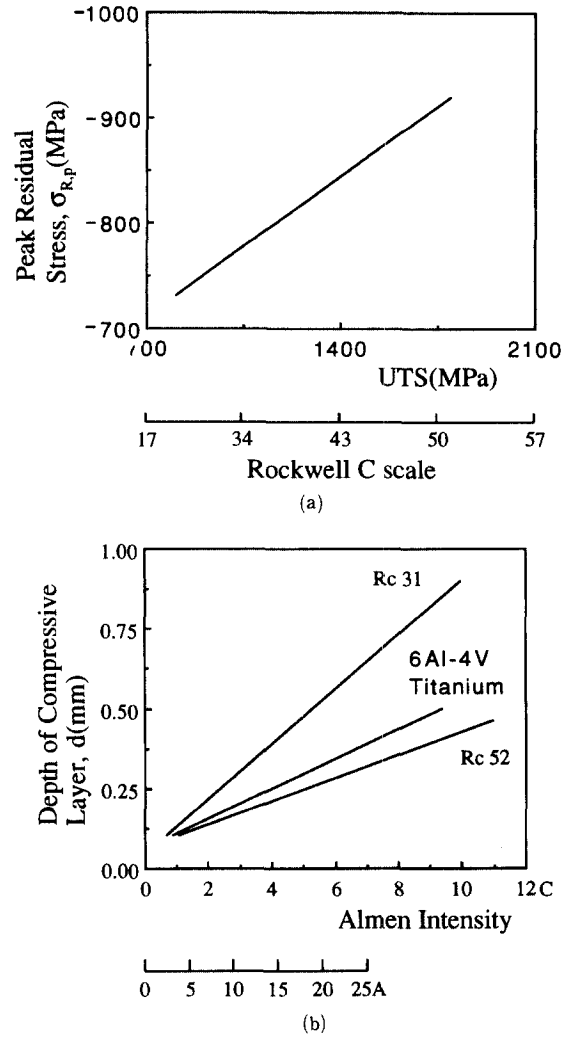

Fig. 7 (a) Maximum compressive residual stress versus ultimate tensile strength and hardness (Shot peening Applications, 1980)
(b) Depth of compressive layer versus peening intensity, A and C indicate the Almen Intensity Scale (Fuchs, 1981)

cal approach were in good agreements with the finite element analysis.

3. RESIDUAL STRESS DISTRIBUTIONS

The knowledge of the distributions of residual stresses from overloads, thermally induced residual stresses, and mechanically induced residual stresses is impoprtant to obtain the optimal beneficial effects by surface treatments. Information on residual stress distributions is more difficult to find. Only residual stresses produced by overloading can be computed from the loads, the geometry, and the material properties (Gerber and Fuchs, 1970, Heller et al.,1964, Underwood and Kendall, 1984, Dietrich and Potter, 1977). The distributions of residual stresses produced by thermal treatments are very important but difficult to compute and rarely published (Horger, 1950, Mattson & Robinson, 1965, Sharma et al., 1979, Vasilakis, 1986).

Distributions of mechanically produced residual stresses are not quite so rare. Good examples are the work by Niku-Lari(1981) and Fuchs(1984, 1987), the report by Brodrick(1955).

Fatigue strength improvement by shot peening has been so far an experimental nature. The analytical approach involve very complicated procedure. Almen intensity is not sufficient measure for shot peening, a plastic height by shot peening and many other parameters are needed to find the residual stress distributions analytically (Al-Hassani, 1981). However, for the first approximation Fuchs(1988) assumed that these distributions are parabolic, with the peak of the parabola at 1/4 of the total depth to which the compressive stress extends; that this depth is equal to the width of the impression created by the peening balls or by rollers; and that the peak compressive stress equals half of the strain hardened yield strength. According to the assumption, the residual stress

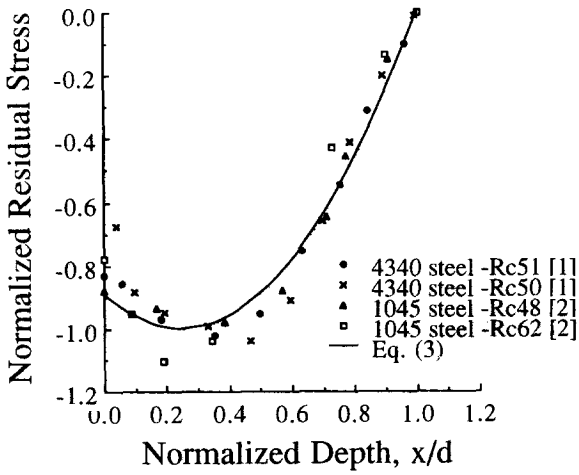

Fig. 8 Comparisons between Eq.(3) and data on dimensionless residual stress distributions of steels after shot peening, AISI 4340 steel is Ni-Cr-Mo alloy steel equivalent to JIS SNCM8 steel, AISI 1045 steel is equivalent to SM45C carbon steel. [1]:(Brodrick, R.E.,1955), [2]:(Lauchner,E., 1974)

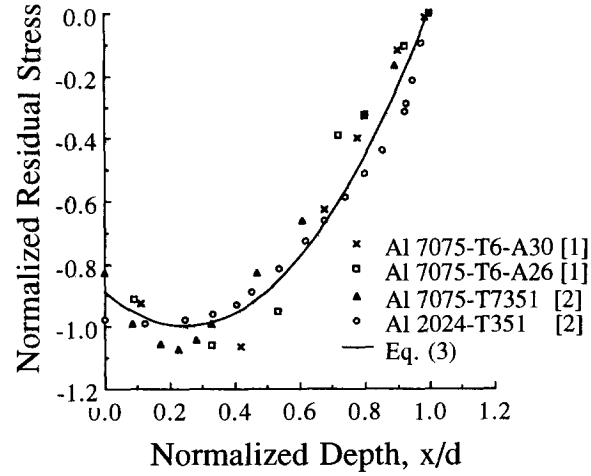

Fig. 9 Comparisons between Eq.(3) and data on dimensionless residual stress distributions of Aluminum Alloy after shot peening.[1]:(Waisman,J.L.,1952), [2] : (Niku-Lari,A.,1984)

distributions by shot peening can be written as following

$$\sigma_R=\sigma_{R,P}\left[1-\frac{(4x/d-1)^2}{9}\right] \tag{3}$$

where $\sigma_{R,P}$ is the maximum compressive residual stress or peak compressive stress, d is the total depth to which the compressive stress extends, and x is same as in Fig. 2.

Fig. 7(a) shows the maximum compressive residual stress versus ultimate tensile strength and hardness and Fig. 7(b) shows the relation between the peening intensity and the depth of compressive residual stress for several materials.

Residual stress distributions of various metals after shot peening are compared with the residual distribution by the empirical formula of Eq. (3). Fig. 8 shows the comparisons between Eq. (3) and data on dimensionless residual stress distributions of steels after shot peening. Residual stress distributions of 4340 steel (Ni-Cr-Mo alloy steel and equivalent to JIS SNCM8 steel) with two different hardness steel measured by Brodrick(1955) and residual stress distributions of 1045 steel (equivalent to SM45C carbon steel) with two different hardness measured by Lauchner(1974) are shown in Fig. 8. Residual stress distribution was normalized by the peak compressive stress. Fig. 9 shows the dimensionless residual stress distributions of aluminum alloys measured by Waisman(1952) and Niku-Lari(1984) and their comparisons with the Eq. (3). Fig. 10 shows the dimensionless residual stress distributions of titanium alloys measured by Leverant(1979) and Braski(1966) and their comparisons with the Eq. (3). As shown in Figs. 8, 9, and 10, various experimental data validated the Eq. (3) as a good formula for the residual stress distribution. Since the depth of compressive stress and the peak compressive stress are available in the literature (Brodrick, 1955) and Fig. 7(a) and Fig. 7(b), the residual stress distribution by shot peening can be obtained by Eq. (3).

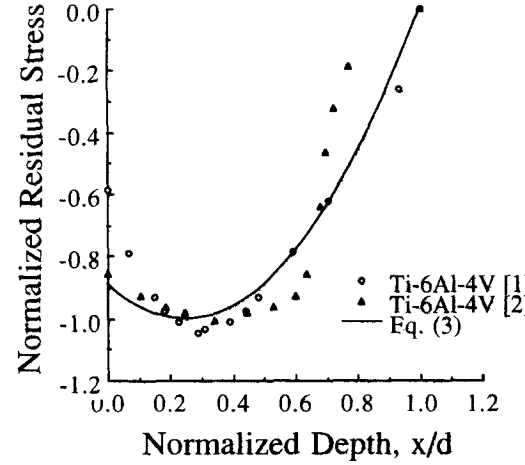

Fig. 10 Comparisons between Eq.(3) and data on dimensionless residual stress distributions of Titanium alloys after shot peening.[1]:(Leverant, G.R.,1979), [2] : (Braski,D.N.,1966)

At notches these residual stresses are also concentrated, but less than the load stresses, as shown by Todd(1971). This stress concentration is usgally neglected.

4. APPLICATIONS AND DISCUSSIONS

4.1 Strength Enhancements by Optimizing the Prestress Treatments

Fig. 11 shows distributions of bending load stress, of shot peening residual stress, of the net stress, and of the local fatigue strength along the depth of the filleted shaft of AISI 4340 steel. The fatigue limit 552 MPa and the mean stress coefficient -0.35 were taken from MIL HDBK 5 (1976) for AISI 4340 steel. The local fatigue strength can be obtained from the fatigue limit with the mean stress like effect of the local compressive residual stress. The net stress is the sum of the load stress and the residual stress. The net stress at the subsurface can be higher than the net stress at surface. Following set of distributions shown in Fig. 11 is one of many computed to find the optimum peening intensity.

Load stress: $\sigma_L=900[0.9(1-x/R)+1.1(1-x/R)^{30.2}]$ (MPa)
Residual stress: $\sigma_R=-876[1-(4x/0.38-1)^2/9]$ (MPa)to $x=0.8$ mm and balanced by tension below d=0.38 mm.

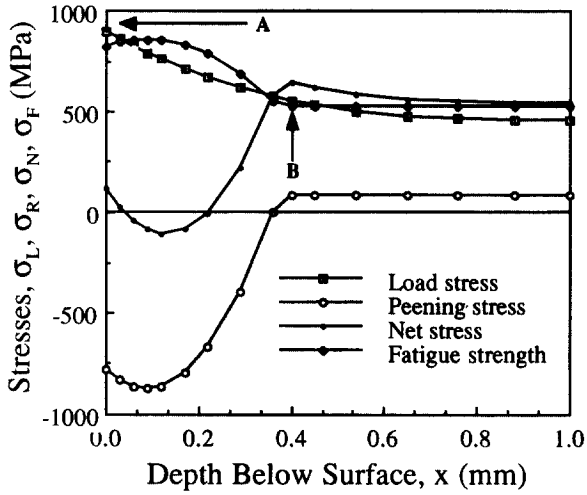

Fig. 11 Stress distributions near a shot peened fillet of a shaft in bending.

Fatigue strength: $\sigma_F = 552 - 0.35\sigma_m = 552 - 0.35\sigma_R$ (MPa)
Net stress: $\sigma_N = \sigma_L + \sigma_R$ (MPa)

Obviously, fatigue cracks only develop where the local load stress is higher than the local fatigue strength. According to Fuchs(1988), the criterion for optimum peening intensity is the equality of risks of failures which start from the surface or from the interior. This residual stress produced by the shot peening is high enough to arrest cracks started at the surface by a high bending load, but not so high that it would start cracks below the surface where the equilibrating tensile residual stress decreases the fatigue strength. Cracks starting at the location A will be arrested by the compressive net stress near x=0.15 mm. Cracks starting at the location B can propagate inwards.

Fuchs(1988) validated his criterion for optimum peening intensity by comparing the conventional peening to optimized peening which was four times as heavy as the conventional treatment. He verified the much greater fatigue resistance of parts treated with optimized peening by tests with shot peened filleted shafts with the large diameter of 25.4 mm, the small diameter of 20 mm, and fillet radius of 0.9 mm.

4.2 Application to Life Predictions

Fatigue life and failure location of shot peened part can be predicted by a damage parameter which is incorporated with material properties, residual stress distributions and load stress distributions. According to SAE Handbook(1983), the generally accepted fatigue life equation for the shot peened parts in high cycle fatigue region can be written as

$$2N_f = \left(\frac{\sigma_a}{\sigma_f' - \sigma_m - \sigma_R} \right)^{\frac{1}{b}} \quad (4)$$

where N_f is the number of cycles to failure, σ_a is the alternating load stress($=\sigma_L$), σ_f' is the fatigue strength coefficiendnt, σ_m is the mean load stress, σ_R is the residual stress and b is the fatigue strength exponent. The damage parameter is proportional to the ratio of the load stress and the fatigue stength. Fatigue cracks will start at locations A and B in Fig. 11 where the damage parameter is high because the higher damage parameter corresponds to the shorter fatigue life. Starker(1979) et. al reported the subsurface crack initiation during fatigue as a resulft of residual stresses. They showed that cracks at surface are arrested and cracks at the subsurface propagate. Their experimental results can be successfully explained with the distributions shown in Fig. 11.

The residual stress affects the fatigue strength of metals in both crack initiation phase and crack propagation phase. The compressive residual stress reduces the crack initiation because it mitigates or eliminates the fatigue strengh reduction factor as shown in Fig. 1 and also enhances the fatigue strength of materials. The compressive residual stress may arrest cracks by producing compressive net stress under cyclic loading.

Residual stress will be relaxed under cyclic load stress (Morrow et al., 1960) but the relaxation of residual stress will be negligible if the summation of load stress and residual stress is below the yield strength. The amount of the relaxation of residual stress due to the high alternating load stress are well discussed by Fuchs(1982).

The stresses below the surface of notches are of course multi-axial. If one wants to consider all three principal stresses one can calculate an equivalent stress for the early of crack formation, but for crack propagation the largest tensile stress is still the most suitable criterion.

5. CONCLUSIONS

For fatigue strength improvement one should consider the distributions of the load stresses and of the residual stresses which may be used to enhance fatigue resistance. A simple formula for applied load stress distributions at notches was suggested. Factors in the formula for the load stress distributions were found with stress concentration factor and stress gradient and notch geometry. Load stress distributions at notches obtained by the formula were in good agreement with the result by finite element methods for plates and shafts with semi-circular notches under various loadings.

A simple parabolic formula for the residual stress distributions by shot peening was suggested. The residual stress distributions by the formula were also in good agreement with available experimental data. An example of optimum surface treatments and life prediction with damage parameter by using the proposed stress distributions were shown.

ACKNOWLEDGEMENTS

This research was supported by the Korea Science and Engineering Foundation. Prof. Fuchs contributed significantly in the early stage of the research and provided an invaluable guidance. Mr. Jae-Chull Lee performed the finite element analysis.

REFERENCES

Al-Hassani, S. T. S., 1981, Mechanical Aspects of Residual Stress Development in Shot Peening, ICSP CETIM Pergamon Press, pp. 583~602.

Almen, J.O. and Black, P.H., 1963, Residual Stresses and Fatigue in Metals, McGraw-Hill Co., New York.

Berkovitas, A., 1986, "Variation of Fatigue Notch Factor With Lifetime, Stress Ratio and Temperature," J.of Engineering Materials and Technology, Trans. ASME, Vol.108, pp. 179~185.

Braski, D.N. and Royster, D.M., 1966, "X-Ray Measurement of Residual stress in Titanium Alloy Sheet," in J.B. Newkirk and G.R. Mallett, ed., Advances in X-Ray Anaysis, Vol. 10, pp. 295~310.

Brodrick, R.F., 1955, "Protective Shot Peening of Propellers," WADC Tech. Report 55-56, U.S. Dept. of Defense, pp. 306~309.

Dietrich, G. and Potter, J., 1977, "Stress Measurements on Cold Worked Fastener Holes," Advances in X-Ray Analysis, Vol. 20, pp. 321~328.

Fuchs, H.O., 1972, "Regional Tensile Stress as a Measure of the Fatigue Strength of Notched Parts," Mechanical Behavior of Materials, Vol. 2, Society of Materials Science, Kyoto, Japan, pp. 478~488.

Fuchs, H.O., 1981, "The Strength of Shot Peened Parts, Design Calculations and Specifications," Niku-Lari, A. ed., Shot Peening, Proc. 1st Intnl. Conf., Pergamon Press, pp. 323~332.

Fuchs, H.O., 1982, "The Effect of Self Stresses on High Cycle Fatigue," J of Testing and Evaluation, JTEVA, Vol.10, No.4, pp. 168~173.

Fuchs, H.O., ed., 1984, Shot Peening. Proc. 2nd Intnl. Conf. SAE Warrendale PA.

Fuchs, H.O., ed., 1987, Shot Peening Stress Profiles Metal Improvement Co. Paramus, NJ.

Fuchs, H.O., 1988, "Approximate Analysis for Optimizing Prestress Treatments," Analytical and Experimental Methods for Residual Stress Effects in Fatigue, ASTM STP 1004, R.L. Champoux, J.H. Underwood, and J.A. Kapp, Eds., American Society for Testing and Materials, Philadelphia, pp. 13~20.

Gerber, T.L. and Fuchs, H.O., 1970, "Improvement of the Fatigue Strength of Notched Bars by Compressive Self-Stresses," Achievement of High Fatigue Resistance in Metals and Alloys, ASTM STP 467, pp. 276~295.

Heller, R.A., Seki, M. and Freudenthal, A.M., 1964, "The Effects of Residual Stress on Random Fatigue Life," Proceedings ASTM, Vol.64, pp. 516~535.

Horger, O.J., 1950, "Residual stresses," ch.11 in Hetenyi, M. ed. Handbook of Exp. Stress Analysis, John Wiley & Sons, New York, pp. 459~578.

Klesnil, M. and Lukas, P., 1980, Fatigue of Metallic Materials Science Monographs, Vol. 7, Elsevier Scientific Publishing Co., pp. 187~188.

Lauchner, E., 1974, "Peening of High Strength Steel Using Hard Shot," Presentation at WESTEC.

Leverent, G.R., Langer, B.S., Yuen, A. and Hopkins, S.W., 1979, "Surface Residual Stresses, Surface Topography, and the Fatigue Behavior of Ti-6Al-4V," Metallurgical Trans, Vol. 10 A. pp 251~257.

Mattson, R.L. and Robinson, G.H., 1965, "Case Carburizing," in Horger, O.J. ed. Metal Engineering-Design, McGraw-Hill, New York, pp. 284~290.

MIL-HDBK-5C, 1976, Metallic Materials and Elements f. Aerospace Structures, U.S. Dept. of Defense, pp. 3~284.

Morrow, J., Ross, A.A., and Sinclair, G.M., 1960, "Relaxation of Residual Stresses Due to Fatigue Loading," SAE Trans. Vol. 68, p. 40.

Neuber, H., 1946, Theory of Notch Stresses, J.W. Edwards, Ann Arbor MI.

Niku-Lari, A. ed., 1981, Shot Peening, Proc. 1st Intnl. Conf., Pergamon Press.

Niku-Lari, A., 1984, "Contraintes Residuelles et Fatigue d' aluminium des Alliages Grenailles," in Proceedings, 2nd Intnl. Conf. on Shot Peening, ICSP-2, H.O.Fuchs ed., pp. 102~114.

Peterson, R.E., 1974, Stress Concentration Factors, John Wiley, New York.

Peterson, R.E., 1961, "The Role of Stress Distribution in Fatigue," Experimental Mechanics, Vol. 1, No.4, pp. 105~115.

Roark, R. J. and Young, W.C., 1975, Formulas for Stress and Strain, 5th ed., McGraw-Hill Co., pp. 590~606.

SAE Handbook, 1983, "Technical Report on Fatigue Properties," SAE J 1099, Society of Automotive Engineers, pp. 3.57~3.65.

Schijve, J., 1980, "Stress Gradients Around Notches," Fatigue of Engineering Materials and Structures, Vol.3, No.4, pp. 325~338.

Sharma, V.K., Walter, G.H. and Breen, D.H., 1979, "Predicting Case Depth for Gears," Product Engineering, p.49.

Shot Peening Applications, 1980, 6th ed., Metal Improvement Co., Inc. Paramus, NJ.

Siebel, E. and Stieler, M., 1955, "Non-uniform Stress Distribution in Fatigue," (in German) VDI-Zeitschrift, Vol. 97, No.5. pp. 121~126.

Smith, K.N. Watson, P. and Topper, T.H., 1970, "A Stress-strain Function for the Fatigue of Metals," J. of Materials, Vol.5, No.4, pp. 767~778.

Starker, P, Wohlfahrt, H. and Macherauch, E., 1979, "Subsurface Crack Initiation During Fatigue as a Result of Residual Stresses," Fatig. of Eng. Matl. and Structures, Vol. 1, pp. 319~327.

Todd, R.H., 1971, Self Stress Concentrations. Dissertation, Stanford University. (1970) Also Experimental Mechanics, Vol.11, No.12, pp. 548~553.

Underwood, J.H. and Kendall, D.P., 1984, "Fracture Analysis of Thick-wall Cylinder Pressure Vessel," Theor. & Applied Fracture Mechanics, Vol.2, pp. 47~58.

Vasilakis, J.D., 1986, Thermal and Transformation Stresses in.. Tubes, First Army Conference on Applied Math., George Washington University.

Waisman, J.L., 1952, Report from Technical Service Co. to Metal Improvement Co.

Walker, K., 1970, "The Effect of Stress Ratio During ····· Fatigue," ASTM STP 462, Am.Soc.for Testing and Materials, Philadelphia PA, pp. 1~14.

APPENDIX

Parameters in Load Stress Distributions

The four parameters a, b, c, and n in Eq. (2) are calculated to match the stress concentration factor at the surface, the stress gradient at the surface, and equilibrium with the nominal stress distribution, and the stress condition at the center, i.e., $\sigma_L|_{x=R}=0$ for bending or torsion, $d\sigma_L/dx|_{x=R}=0$ for tension or for the plate under out-of-plane bending. The calculated parameters for various cases follow.

- a plate loaded in tension or out-of-plane bending

$$a=(w/\eta+1-K_t)/(w/\eta-1+1/K_t)$$

$b=0$

$$c=K_t-a$$

$$n=(K_t-1)/(1-a) \qquad \text{(A1)}$$

- a plate subject to in-plane bending

$$a=0$$

$$b = K_t \cdot c$$
$$c = (K_t\text{-}1)(n+1)/(n\text{-}1)$$
$$n = \{(w/\eta - 2)K_t + 1)\}/(K_t - 1) \quad \text{(A2)}$$

• a shaft loaded in tension

$$a = \{(R/\eta + 2(1-K_t)\}/\{(R/\eta - 2(1-1/K_t)\}$$
$$b = 0$$
$$c = K_t \cdot a$$
$$n = 2(K_t\text{-}1)/(1\text{-}a) \quad \text{(A3)}$$

• a shaft loaded in torsion

$$a = 0$$
$$b = K_t \cdot c$$
$$c = (K_t\text{-}1)(n+2)/(n\text{-}1)$$
$$n = \{(R/\eta - 3)K_t + 2\}/(K_t - 1) \quad \text{(A4)}$$

• a shaft loaded in bending

$$a = 0$$
$$c = K_t \cdot c$$
$$n = (R/\eta - 1)K_t/(n-1) \quad \text{(A5)}$$

n should be obtained numerically

These factors are good for plates or shafts with semi-circular notches or quarter-circular fillets with different values of K_t and η, which can be obtained by finite element methods or from the literatures; K_t in (Peterson, 1974; Roark and Young, 1975) and η in (Siebel and Stieler, 1955, Klesnil and Lukas, 1980).